

Local order of the high-pressure metallic phase of liquid selenium: a diffraction study

This article has been downloaded from IOPscience. Please scroll down to see the full text article.

1999 J. Phys.: Condens. Matter 11 10243

(<http://iopscience.iop.org/0953-8984/11/50/316>)

View [the table of contents for this issue](#), or go to the [journal homepage](#) for more

Download details:

IP Address: 171.66.16.218

The article was downloaded on 15/05/2010 at 19:12

Please note that [terms and conditions apply](#).

Local order of the high-pressure metallic phase of liquid selenium: a diffraction study

J Y Raty[†]||, J P Gaspard[†], T Le Bihan[‡], M Mezouar[‡] and M Bionducci[§]

[†] Condensed Matter Physics B5, University of Liège, B-4000 Sart-Tilman, Belgium

[‡] European Synchrotron Radiation Facility, BP220, F-38043 Grenoble, France

[§] Léon Brillouin Laboratory, CEA-CNRS, F-91191 Gif-sur-Yvette Cédex, France

Received 20 August 1999, in final form 29 September 1999

Abstract. Liquid selenium undergoes a phase transition towards a metallic phase when sufficient pressure is applied. We performed an x-ray diffraction experiment at the ID30 beamline of the ESRF at the wavelength of 0.149 Å to investigate the local order of the metallic liquid. The diffraction pattern of liquid Se has been recorded with the large-volume Paris–Edinburgh cell between (20 °C, 3 GPa) and (1650 °C, 4.1 GPa). The local order of the metallic liquid selenium is found to be close to that of liquid tellurium. In particular, the coordination number Z increases with temperature from 2.6 to 3.0.

1. Introduction

The structure of selenium has been the subject of a considerable number of studies as selenium is an elemental system that undergoes a phase transition towards a metallic state under pressure and at elevated temperatures. The comparison with Te, its heavier analogue, is of considerable importance for the understanding of the chemical bond and its evolution with increasing temperature and pressure

The phase diagram of selenium, shown in figure 1, has been determined on the basis of resistivity measurements and differential thermal analysis [1]. The crystalline structure is formed of covalent chains of twofold-coordinated atoms. At room pressure, selenium melts without variation of the coordination number, transforming into the phase L. At higher temperature, at about 1500 °C and at the pressure of 1 GPa, the liquid becomes a metallic conductor (phase L'). A triple point occurs at 3.6 ± 0.5 GPa and 900 ± 30 K. The L–L' coexistence line has a negative slope dT/dP similarly to water and the elemental or compound semiconductors (Si, Ge, GaAs, ...). This negative slope is associated with a drastic change in the physical properties, usually a semiconductor-to-metal transition, that must be related to noticeable structural changes.

Some structural data are available on liquid Se for high pressure (>4.4 GPa) and temperatures below 1000 K [2–4]. The observation of the x-ray spectra [2] indicates, for the liquid at $P > 4$ GPa, a qualitative resemblance with those of liquid Te. Recent EXAFS measurements [4] show a tendency for the average distance between first neighbours to increase when pressure is applied. In this paper we analyse the coordination number and interatomic distances in Se in the pressure range of 2.9 to 4.1 GPa, from room temperature up to 1650 °C,

|| Author to whom any correspondence should be addressed.

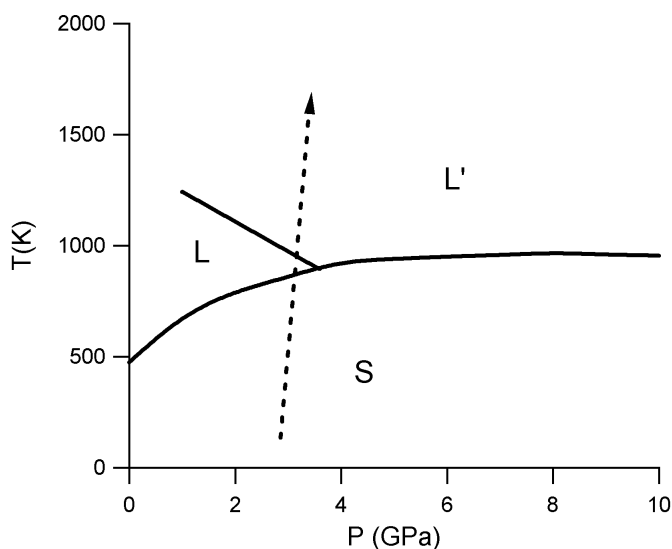


Figure 1. The (P, T) equilibrium phase diagram of selenium. S is the semiconducting crystalline phase, L is the semiconducting liquid and L' is the metallic liquid. The dotted line represents the locus of the experimental points.

following the dotted line of figure 1, to detect the structural changes that can take place in the L region of the phase diagram.

2. Data collection and treatment

The experiment has been performed on the ID30 beamline of the European Synchrotron Radiation Facility (ESRF), Grenoble. The beam energy can be varied from 20 keV to 85 keV with a double Si(111) monochromator. We select an energy as high as $E = 82.818$ keV, corresponding to a wavelength $\lambda = 0.149$ Å, to scan a wide range of q -values and achieve sufficient transmission through the high-pressure apparatus. The dimension of the spot impinging on the sample is $10 \text{ mm} \times 10 \text{ mm}$.

The high-pressure–temperature device is the Paris–Edinburgh large-volume cell [5], which permits one to apply a pressure up to 10 GPa and to reach a temperature of about 1700 K. The pressure is generated by a hydraulic pump compressing a boron nitride gasket between two tungsten carbide anvils. The sample, a finely ground amorphous Se powder, is compressed in a fine-bore nitride cylinder ≈ 2 mm in diameter, and 4 mm in height, which is heated by the Joule effect in a cylindrical graphite oven, 2 mm in diameter and 1 mm in thickness, surrounding the sample holder.

The experiment was realized in transmission geometry, the spectra being registered on an optically read bi-dimensional image plate (Fastscan prototype; for details, see [6]). The intensity collected on the image plate is averaged over a constant diffraction angle, 2θ , to give a unidimensional spectrum, $I(2\theta)$. The aberrations arising from geometrical misalignment effects on the image plate are corrected during the averaging procedure.

Two measurements were performed at each (P, T) point, corresponding to the intensity diffracted by the sample + container and from the container alone. Each data collection took about two minutes and 30 (P, T) points were investigated on the dotted line traced in figure 1. The data have been corrected for the efficiency profile of the image plate and for the absorption, to give the intensity diffracted by the sample alone, I_S . The intensities were then scaled to atomic units by high-angle normalization to the Se atomic form factor, $f(q)$. The resulting

structure factor, $S(q)$, is therefore given by

$$S(q) = \frac{I_S(q)}{\alpha f(q)} - C(q) \quad (1)$$

where $C(q)$ is the Compton scattering contribution and α is the scaling factor.

The cell is, in principle, subjected to a constant pressure throughout the complete data collection. In practice, the dilation of the cell components makes the effective pressure on the sample become higher with temperature increase. The pressure and temperature corresponding to a given data collection are determined in an indirect way, by checking the variation with P and T of the lattice parameters in the crystalline boron nitride and in a platinum microcrystal placed between the sample holder and the furnace. By means of the known state equation $V(T, P)$ of the two materials, the experimental P and T can be calculated from the intersection of two isochores. The calculated values of P , T are reported in figure 2. The precisions of the calculated P , T are of the order of 0.5 GPa and 10%, respectively.

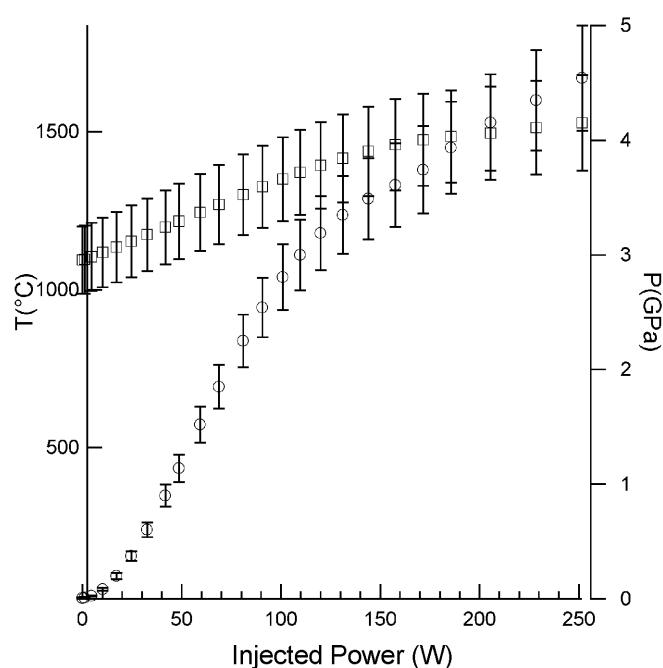


Figure 2. Calculated pressure (squares) and temperature (circles) values, corresponding to the experimental conditions (the dotted line in figure 1), versus injected power.

3. Results

Figure 3 shows some of the spectra collected during the experiment, after data reduction. The structure factors 1–3, corresponding to $T = 20$ – 93 °C, are typical for the amorphous structure of Se. From the patterns 4 and 5, it is clear that between 93 °C and 160 °C the crystallization of the sample takes place (the amplitudes of the highest peaks are reduced for clarity).

Melting occurs between 570 °C and 700 °C, as can be deduced from the progressive decrease in height and broadening of the Bragg peaks. After the phase transition, the main effect on all of the peaks is the decreasing of the peak heights with increasing temperature. The last structure factor ($P = 4.1$ GPa, $T = 1650$ °C) presents only a broad structure, the high-frequency oscillation representing a residual diffraction coming from a different part of the apparatus.

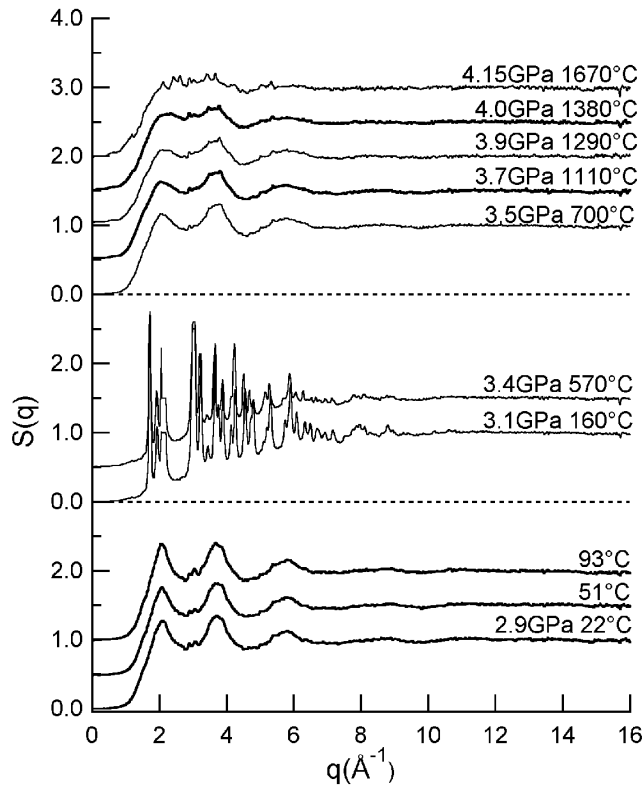


Figure 3. Structure factors of Se at different P , T points. Bottom three curves: amorphous phase; next two curves: crystalline phase (the third and fourth peaks are reduced in height to improve readability); the other curves were collected in the region L.

The pair correlation functions $g(r)$, plotted in figure 4, were obtained by Fourier transforming the $S(q)$ of figure 3, according to the relationship

$$g(r) = 1 + \frac{1}{2\pi^2\rho r} \int q(S(q) - 1) \sin(qr) dq \quad (2)$$

where the number densities ρ were measured in the range of P , T for the solid phase by Katayama [7].

Again, the $g(r)$ of the amorphous and the first spectrum for the liquid are very similar, with comparable first and second peaks. With increasing temperature, the first peak is gradually smeared out while the hollow minimum between the first and second peaks fills in.

The $g(r)$ corresponding to the crystallized Se have been calculated in the same way as the ones for the amorphous and liquid Se. The delta peaks are enlarged by the resolution effects intrinsic to the experimental apparatus, as well as by the upper limitation of the data in the reciprocal space. The number of neighbours in the first shell, Z , calculated by the integration of $g(r)$ up to its first minimum, is very close to its actual value of 2 for all of the data collected between 160 °C and 570 °C (figure 5), while the Se–Se first distance is $r = 2.38$ Å when $T = 160$ °C, and increases continuously to $r = 2.42$ Å when $T = 570$ °C, following the thermal expansion of the solid. The value of Z is completely consistent with the known twofold-coordinated chain structure of crystalline Se, allowing us to evaluate the accuracy of the data treatment. This also shows that, in favourable cases, the treatment of the diffraction pattern for a crystal in the same manner as that for a liquid can give indications as to the local ordering inside the crystal.

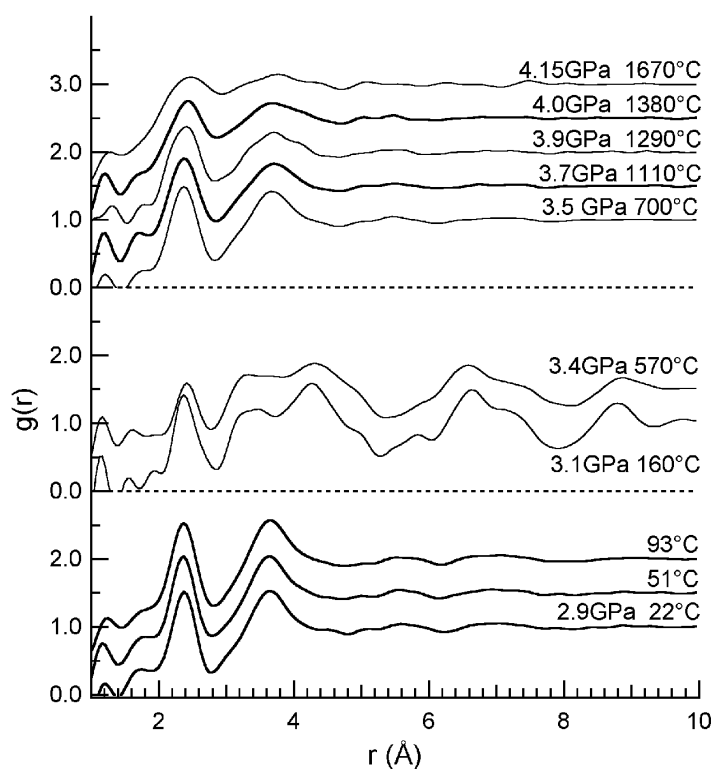


Figure 4. Pair correlation functions corresponding to the structure factors of figure 3.

4. Discussion

The evolution of Z (figure 5) shows interesting features. First, Z is almost equal for amorphous Se and the lowest-temperature (LT) liquid, despite the thermal expansion. With the rise of temperature, Z increases from 2.6 at 600 °C to 3 at 1600 °C. It is worth noting that, if we neglect the middle zone of figure 5, corresponding to the temperatures where crystallization occurs, the evolution of Z is almost linear with temperature. The values of Z reported here are very similar to those measured for liquid tellurium (under saturated vapour pressure), with the same evolution in temperature. In the case of tellurium, the structure has been shown [8] to be an entanglement of Te chains, with a degree of branching rising with T . This consideration, combined with the fact that the Se structure factors recorded during this experiment are also similar to those of liquid tellurium, leads to the conclusion that it seems probable that the structure of liquid Se in the metallic phase L' consists of entangled chains. The liquid can be pictured as a mixing between twofold-coordinated atoms involved in chains and threefold-coordinated atoms ensuring the connection between those chains.

The first-neighbour distance, r_1 , is also similar for the amorphous and the LT liquid despite the thermal expansion. It does not evolve noticeably in the amorphous phase either (see figure 6). This indicates that the effect of thermal expansion is to separate the chains from each other rather than modifying the chain structure. Indeed, simple calculations (using the model described in reference [9]) can show that, at constant T , a higher separation between chains induces a slight shortening of r_1 . For the liquid, the curve $r_1(T)$ is quite parabolic. This effect is due to several contributions (we neglect the slight variation in density due to

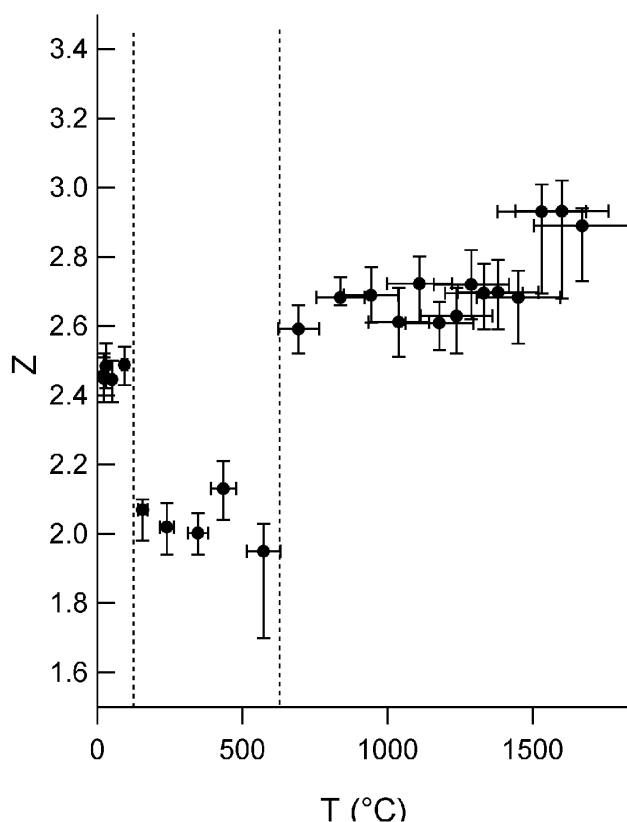


Figure 5. Evolution of the coordination number, Z , versus temperature. The pressure range is 2.9 GPa up to 4.1 GPa. The dotted lines represent the amorphous–solid–crystalline–liquid phase transitions.

the increasing effective P): (i) the growth of Z also contributes to the increase in r_1 ; (ii) the thermal expansion acts more and more on a network rather than on chains, the result being to enlarge the average r_1 .

5. Conclusions

In this paper we have analysed the structural properties of selenium at high pressures, between 2.9 and 4.1 GPa over a broad range of temperatures. The detailed description of the liquid structure is beyond the scope of this paper and will be the subject of a forthcoming paper where the model constructed in [9] will allow us to discuss the effect of coordination defects and of the degree of branching of chains in the liquid with respect to the electrical conductivity. However, we have shown that the high-quality spectra recorded, and the comparison with earlier work on Te, suggest that a high number of interconnected chains exist in liquid Se, the interconnection rate increasing with temperature. We also show that the amorphous structure under pressure has a strong similarity with the structure of the liquid. An interesting similarity is found between high-pressure selenium and tellurium at room pressure. This was already observed in computer simulation, where the density has been shown to be a key parameter [9].

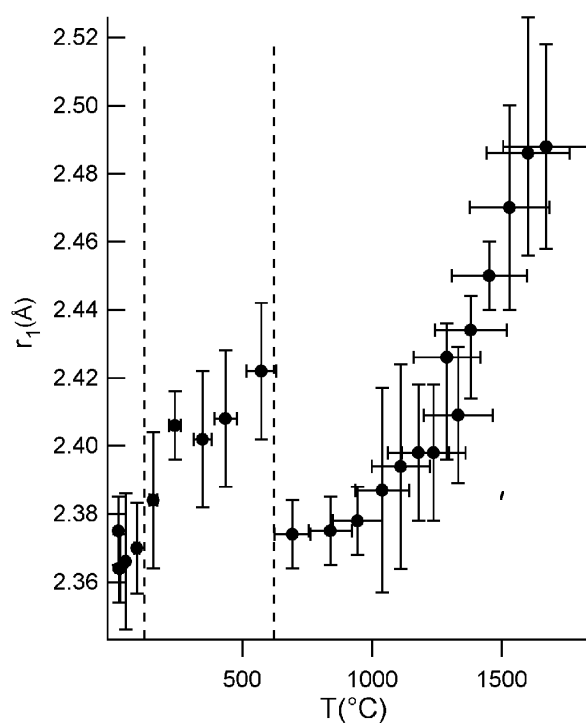


Figure 6. Evolution of the first-neighbour distance, r_1 , versus temperature. The pressure range is 2.9 GPa up to 4.1 GPa. The dotted lines represent the amorphous–solid–crystalline–liquid transitions.

Acknowledgment

We gratefully acknowledge Dr Y Katayama for providing us with the crystal density data. This work was supported by the FNRS (grant FRFC 2.4515.90).

References

- [1] Brazhkin V V, Voloshin R N and Popova S V 1990 *JETP Lett.* **50** 425
- [2] Tsuji K, Shimomura O, Tamura K and Endo H 1988 *Z. Phys. Chem., NF* **156** 495
- [3] Tsuji K, Yamamoto Y, Katayama Y and Koyama N 1993 *High-Pressure Science and Technology* ed S C Schmidt, J W Shaner, G A Samara and M Ross (New York: AIP) p 311
- [4] Katayama Y, Tsuji K, Oyanagi H and Shimomura O 1998 *J. Non-Cryst. Solids* **232–234** 93
- [5] Mezouar M, Le Bihan T, Libotte H, Le Godec Y and Hausermann D 1999 *J. Synchrotron Radiat.* at press
- [6] Thoms M, Bauchau S, Kunz M, Le Bihan T, Mezouar M, Hausermann D and Strawbridge D 1998 *Nucl. Instrum. Methods A* **413** 175
- [7] Katayama Y 1998 private communication
- [8] Bichara C, Raty J Y and Gaspard J P 1996 *Phys. Rev. B* **53** 206
- [9] Raty J Y, Gaspard J P, Saùl A and Bichara C 1999 *Phys. Rev. B* **60** 2441